Discriminative Spectral Regions for Detecting Huanglongbing in Citrus Plants through Statistical Analysis

Mauro Morata Bortoloto Junior [1], Lucas Prado Osco [2], Lúcio Andre de Castro Jorge [3], Ana Paula Marques Ramos [4]

[1&4]Departament of Cartography - São Paulo State University (UNESP), Roberto Simonsen 305, 19060-900, Presidente Prudente, São Paulo, Brazil – [1]mauro.morata@unesp.br; [4]marques.ramos@unesp.br;
[2]Pos-Graduate Program of Environment and Regional Developement – Western São Paulo State (UNOESTE), Raposo Tavares km 572, 19067-175, Presidente Prudente, São Paulo, Brazil - lucasosco@unoeste.br;
[3]Embrapa Instrumentação, Brazilian Agricultural Research Corporation, São Carlos 13560-970, Brazil – lucio.jorge@embrapa.br

Keywords: HLB detection, hyperspectral data, parametric statistical methods, citrus disease, spectral feature selection.

Abstract

This study aims to characterize the spectral reflectance of healthy and huanglongbing (HLB)-infected citrus individuals at both the leaf and plant levels using a statistical approach. Our main contribution is to assess the extent to which hyperspectral measurements can differentiate disease status. Spectral data were collected from 1,912 leaves belonging to 89 citrus plants, of which 29 were found to be infected with HLB and 60 were healthy. A statistical protocol—including Shapiro-Wilk, Welch's t-tests, ANOVA, and Z-tests—was applied to estimate the mean and standard deviation of spectral reflectance for each class, evaluate the spectral variance across bands at the plant level, determine differences between HLB-positive and HLB-negative groups at both hierarchical levels (leaf and plant), and identify the spectral bands with the highest discriminatory power. The findings reveal substantial intra-plant spectral variability in HLB-positive citrus, indicating that individual leaf reflectance may not reliably represent whole-plant disease status. This reinforces the need for plant-level spectral aggregation in remote sensing models. Discriminative spectral intervals were consistently identified in the 400–431 nm, 488–752 nm, 1132–1830 nm, and 1890–2500 nm ranges, spanning the visible to shortwave infrared (SWIR) spectrum.

1. Introduction

Brazil is among the world's leading orange producers and stands as the top exporter of pasteurized orange juice, a sector that plays a vital role in the nation's Gross Domestic Product (GDP). According to the latest report by the United States Department of Agriculture (USDA), the Brazilian orange crop for the 2024/25 season is projected to reach 320 million boxes of 40.8 kg each (approximately 13 million tons), marking a 5.4% increase compared to the 2023/24 season. This modest recovery follows the lowest recorded output since 1988. The production of frozen concentrated orange juice (FCOJ 66 Brix equivalent) is also expected to rise by 8%, reaching 1.0 million tons, driven by an increased availability of fruit for industrial processing (Castro, 2025). The state of São Paulo remains the main production hub, with 357,433 hectares under cultivation and a total output of 13,025,994 tons—accounting for 76.9% of the national production (IBGE, 2022).

Huanglongbing (HLB), also known as citrus greening, is among the most devastating diseases impacting citrus crops globally. It is caused by the bacterium *Candidatus Liberibacter* spp. and primarily transmitted by insect vectors. Traditional detection methods, including visual inspections and molecular techniques, such as PCR (Polymerase Chain Reaction), are hindered by the pathogen's uneven distribution within the host and the absence of visible symptoms during early infection stages. Remote sensing, particularly through hyperspectral data, provides a non-intrusive means of studying HLB, enabling disease monitoring without direct contact with the plants. This approach holds great potential for developing early detection methods, including the identification of asymptomatic infections, before visible symptoms appear. However, despite its promise, no definitive or widely accepted remote sensing-based method for HLB detection has yet been established, highlighting a critical gap to be to be addressed.

To advance efforts in HLB detection, it is essential to characterize the spectral signatures of infected and healthy individuals, as this may enable the identification of specific spectral regions with the highest discriminatory power between the two conditions. Recognizing these spectral regions is crucial for developing automated, non-invasive monitoring tools. Moreover, performing this characterization at both the leaf level and the plant level allows researchers to assess the consistency and reliability of the spectral indicators across different spatial scales. Leaf-level analysis provides insight into localized physiological responses, while plant-level aggregation reflects broader patterns that are more representative of remote sensing applications (Orlando, 2024).

In this context, statistical methods—both parametric and non-parametric—play a central role in supporting robust spectral characterization. Given the high dimensionality of hyperspectral data and the potential non-normality of reflectance distributions across wavelengths, statistical testing offers a rigorous framework to identify spectral signatures that exhibit differences between healthy and diseased samples. Parametric tests, such as the Welch *t*-test or ANOVA, are suitable when data meet normality assumptions, while non-parametric counterparts like the Mann–Whitney *U* test provide reliable alternatives in more flexible settings. These methods not only strengthen the interpretability of spectral differences but also guide the selection of informative spectral regions for downstream classification or disease monitoring.

Given the discussed issue, this study aims to identify discriminative spectral regions for detecting Huanglongbing in citrus plants through statistical analyses conducted at both the leaf and plant levels, evaluating the effectiveness of reflectance data in distinguishing healthy and infected individuals. Our main contribution is to assess the extent to which hyperspectral

This contribution has been peer-reviewed. The double-blind peer-review was conducted on the basis of the full paper.
https://doi.org/10.5194/isprs-annals-X-3-W4-2025-255-2026

measurements can differentiate disease status and support the optimization of remote sensing models for HLB detection in citrus orchards.

Although this study focuses on spectral characterization at the leaf and plant levels, its findings have important implications for remote sensing-based disease monitoring. The identification of robust discriminative bands within the visible, red-edge, and SWIR regions establishes a strong foundation for the development of targeted vegetation indices and the design of optimized sensors for UAV and satellite platforms. By linking spectral patterns to scalable sensing strategies, this study bridges the gap between proximal spectroscopy and operational canopy-level monitoring, strengthening the potential of remote sensing tools for early and efficient HLB detection.

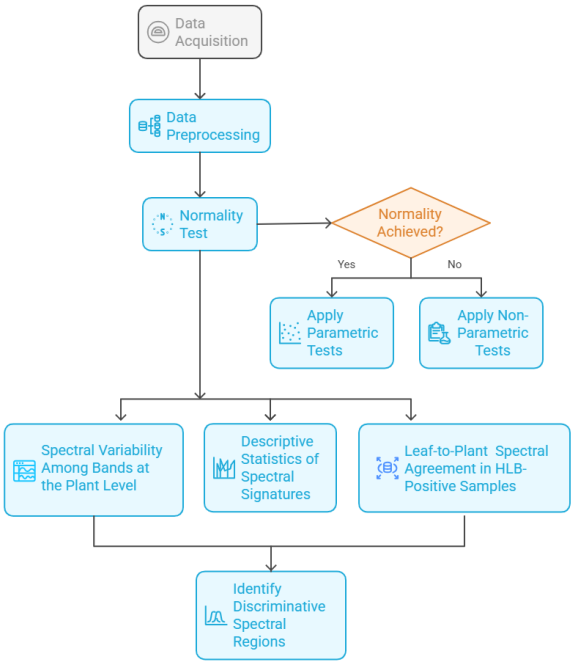

Figure 1 - Workflow summarizing the steps involved in spectral region differentiation for HLB detection. The process includes spectral data acquisition, preprocessing, statistical testing, and the identification of discriminative wavelength ranges for disease classification.

2. Materials and Methods

2.1 Study Area and Sampling

The data consist of hyperspectral measurements collected in orange groves at the Entre Rios farm (FUNDECITRUS) in Boa Esperança do Sul, São Paulo, in 2019. The region's climate is classified as humid subtropical (Cwa) according to the Köppen-Geiger classification, a predominant soil type in their region is Red Latosol, characterized by its depth and high drainage capacity. Subordinate soil types include Red-Yellow Latosols and, in specific areas, Quartzarenic Neosols.

The samples were acquired during the late vegetative phenological stage of the plants, which influences their spectral characteristics. Leaves were collected from the North, South, East, and West sides of the canopy at different heights, with approximately 20 samples per plant. This strategy enabled the detection of HLB symptoms in any part of the canopy, regardless of the infestation level. A total of 89 plants and 1,912 leaves were sampled, distributed across four plots. For each plant, all sampled leaves were ground together and tested using the PCR laboratory method, which indicated the presence or absence of HLB infection. Pera Rio graft onto Tangerine Sunki was the species inspected.

Although the molecular diagnosis was performed at the plant level using pooled leaves, each sampled leaf was considered an independent spectral unit. Therefore, individual spectral measurements were labeled according to the PCR status of the corresponding plant. This procedure allowed us to evaluate intra-plant variability, but we acknowledge that it may introduce bias by including asymptomatic leaves within HLB-positive plants

2.2 Spectral Data Acquisition

Reflectance measurements were obtained using a spectroradiometer operating in the 350–2500 nm range, with each spectral profile representing the average of 10 individual measurements taken per leaf. The dataset is organized in a spreadsheet format, with the following fields: *SAMPLE*, which identifies each individual sample; *LOT*, indicating the plot to which the plant belongs; *STREET*, corresponding to the row in which the plant is located; *PLANT*, identifying the specific plant within the row; *LEAF*, indicating the leaf sampled; and *HLB*, which denotes whether the plant is infected with the disease.

2.3 Data Preprocessing

All negative reflectance values were replaced by zero, and the data were reorganized to associate each sample with a composite plant identifier (LOT + STREET + PLANT). A column labeled HLB was created to indicate the health status of each leaf. Spectral bands were treated as numerical variables for statistical evaluation. During preprocessing, spectral bands corresponding to noisy regions—typically located at the beginning and end of the spectrum, as well as mid-range water absorption features—were removed. As a result, the final dataset retained only valid and reliable spectral reflectance values within the range of 400 to 2450 nm, ensuring cleaner input for statistical analysis.

2.4 Statistical Analysis

Normality of spectral distributions was tested using the Shapiro–Wilk test (Shapiro & Wilk, 1965), applied separately for each plant and leaf group. This test evaluates whether a dataset follows a normal distribution by comparing the ordered sample quantiles with expected quantiles from a Gaussian distribution. It is particularly sensitive for small and medium sample sizes and is widely used in hyperspectral studies to verify the assumption of normality across multiple wavelengths.

To compare reflectance values between HLB-positive and HLB-negative groups, two complementary parametric tests were applied: Welch's t-test (Welch, 1947) and one-way ANOVA (Fisher, 1925). Welch's t-test was selected for the leaf-level analysis because it is robust to heteroscedasticity (unequal variances) and differences in sample size between groups, making it suitable for hyperspectral data where variance can vary across wavelengths**.** One-way ANOVA was applied at the plant level, where aggregation reduced intra-class variance, enabling a more reliable evaluation of differences in mean reflectance between healthy and diseased plants across the spectral range.

https://doi.org/10.5194/isprs-annals-X-3-W4-2025-255-2026

To evaluate the consistency of individual leaf spectra within HLB-positive plants, a single-observation Z-test (Walpole et al., 2012) was used. This test compares the spectral response of an individual leaf against the distribution of a healthy reference group, using the group's mean and standard deviation for each wavelength. This approach enabled the identification of potentially asymptomatic leaves within infected plants, which could otherwise bias model training and classification accuracy.
.

3. Results and Discussion

3.1 Exploratory Statistical Characterization of Spectral Signatures in HLB-Positive and HLB-Negative Samples

To determine the appropriate statistical approach, the normality of spectral reflectance values at each wavelength was evaluated using the Shapiro–Wilk test, applied separately to the datasets aggregated by plant and by individual leaf, figure 2.

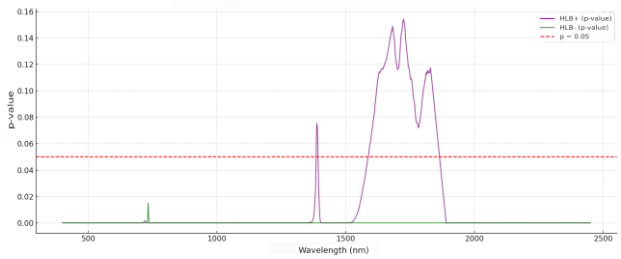

Figure 2 - Results of the Shapiro-Wilk test applied to spectral reflectance data at the leaf level. The figure illustrates p-value distributions across wavelengths, highlighting deviations from normality, particularly in some HLB-positive leaf samples.

The Shapiro-Wilk test revealed that certain spectral bands within the HLB-positive group deviated from a normal distribution. In contrast, HLB-negative plants exhibited more consistent p-values across leaves, indicating a more stable spectral behaviour. At the plant level, most wavelengths conformed to normality assumptions, with only a few plants displaying deviations from the expected distribution pattern. The similarity between mean and median reflectance values across wavelengths—an indicator commonly used to assess distribution symmetry—also supports the normality assumption (Lopes, 2013), explicated at figure 3.

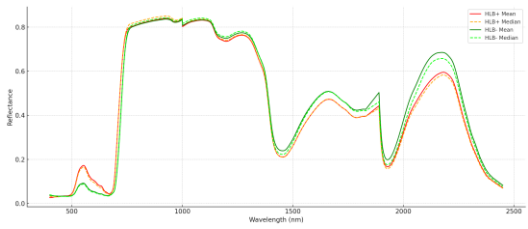

Figure 3 - Comparison between mean and median reflectance values across spectral reflectance at leaf level. The close alignment between these metrics supports the assumption of symmetrical data distribution, especially among healthy plant samples.

Although the Shapiro-Wilk test indicated deviations from normality at certain wavelengths—particularly among reflectance data from HLB-positive leaves. The spectral means aggregated at the plant level closely followed a normal distribution pattern across wavelengths, figure 4. This observation is statistically supported by the Central Limit Theorem (CLT), which validates the use of parametric tests on leaf and plant-level means. Therefore, the plant-level aggregation strategy not only mitigates intra-plant variability but also enhances the statistical robustness of spectral analysis for disease detection. Hereford, parametric methods remain valid for further analysis.

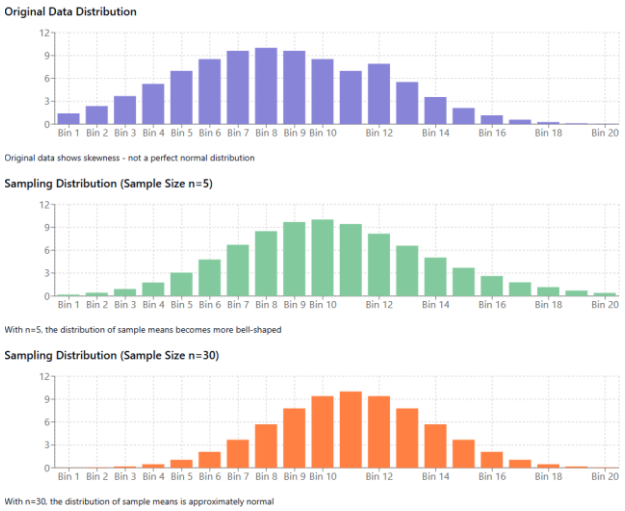

Figure 4 - As sample size increases, the sampling distribution of means becomes increasingly normal, regardless of the shape of the original population distribution. This is the essence of the Central Limit Theorem.

The results presented in Figure 5 illustrate how the Shapiro-Wilk test's sensitivity increases with larger sample sizes, this behavior is a known limitation of the test, as it tends to detect minor deviations from normality in large datasets which can lead to statistically significant p-values ($p < 0.05$) even in cases where the data distribution visually resembles normality, which may not be practically relevant (Razali & Wah, 2011).

This result at figure 5 is likely influenced by the high dimensionality of the dataset and the sensitivity of the test to large sample sizes. Therefore, considering both theoretical foundations and empirical indicators, the dataset can be reasonably assumed to follow a normal distribution for the purposes of parametric analysis.

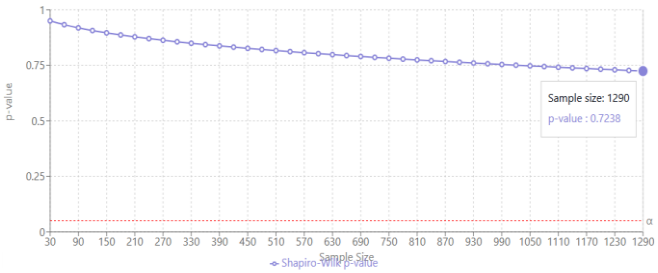

Figure 5 - Variation of the Shapiro-Wilk test statistic across spectral bands for HLB-positive plants. Although the test statistic decreases slightly with increasing sample size, it does not reach the significance threshold ($p < 0.05$) for most wavelengths, indicating that the aggregated spectral data largely satisfy the assumptions of normality required for parametric analysis.

This result at figure 6, highlighting a statistically significant difference in reflectance at 1610 nm between HLB-negative and HLB-positive leaf's, even if individual leaf-level reflectance

This contribution has been peer-reviewed. The double-blind peer-review was conducted on the basis of the full paper.
https://doi.org/10.5194/isprs-annals-X-3-W4-2025-255-2026 | © Author(s) 2026. CC BY 4.0 License.

values do not follow a normal distribution, the distribution of their means approximates normality as the sample size increases. Evaluating plant-level spectral differences and reinforces the robustness of the observed contrast at 1610 nm.

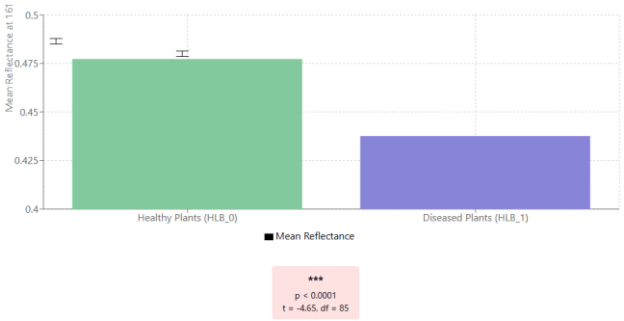

Figure 6 - There is a significant difference in reflectance at 1610 nm between healthy (HLB-) and diseased (HLB+) plants. Healthy plants show higher mean reflectance (0.4773) compared to diseased plants (0.4376).

3.2 Characterization of Spectral Patterns Using Descriptive Statistics

Mean and standard deviation values were used to characterize spectral patterns among leaves and plants. Aggregating data at the plant level enhanced the distinction between healthy and diseased groups, reducing intra-plant variability and improving spectral separability. HLB-negative plants showed lower dispersion, indicating greater physiological uniformity. Figure 7 illustrates the mean spectral reflectance and associated standard deviation for HLB-positive (HLB+) and HLB-negative (HLB−) leaf samples across the full spectral range.

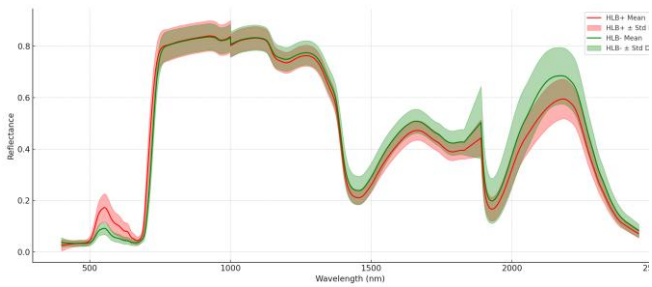

Figure 7 - Mean spectral reflectance and standard deviation for HLB-positive (HLB+) and HLB-negative (HLB−) leaves across the full spectral range.

Figure 8 illustrates the mean spectral reflectance and corresponding standard deviation for HLB-positive (HLB+) and HLB-negative (HLB−) plant samples across the entire spectral range.

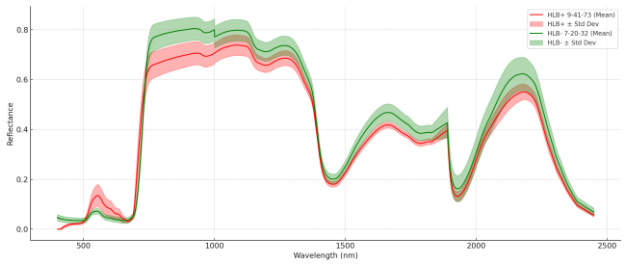

Figure 8 - Mean spectral reflectance and standard deviation of aggregated plant-level data for HLB-positive and HLB-negative plants.

By analyzing figures 7 and 8, it becomes evident that both indicate some similarities. However, within the spectral range from approximately 750 to 1250 nm, the separation between HLB-positive and HLB-negative samples is clearly observed only at the plant level, not at the leaf level. This discrepancy does not necessarily imply that individual leaves are unsuitable for disease detection, but rather may reflect the presence of visually healthy leaves within HLB-infected plants. As mentioned, each plant in the dataset was represented by 20 leaves, and if only one leaf exhibited symptoms while the remaining 19 appeared healthy, all of them would still be labeled as HLB-positive based on the plant-level diagnosis. That's because even though the leaf could appear healthy, they belonged to an infected plant.

In the near-infrared (NIR) region, healthy vegetation typically shows high reflectance due to the backscattering (or multiple scattering) of electromagnetic radiation within the internal structure of the leaf mesophyll. This phenomenon is primarily caused by differences in refractive indices between cell walls, intercellular spaces, and intracellular components, creating multiple interfaces for light dispersion (Jensen, 2009). In contrast, stressed, diseased, or senescent plants exhibit structural alterations—such as cell collapse, reduced mesophyll thickness, or disorganization of the parenchyma—that diminish backscattering and, consequently, reduce reflectance in the NIR (Jensen, 2009). This is one of the main physical principles behind the use of NIR in vegetation indices (e.g., NDVI) and in plant disease detection.

It is important to highlight that some of the observed spectral changes, such as chlorosis, pigment degradation, and variations in leaf water content, are not unique to HLB. Similar responses can arise from nutrient deficiencies, water stress, or other pathogens, leading to overlapping spectral signatures across multiple citrus disorders. This phenomenon of symptom non-specificity has been widely reported in recent studies on hyperspectral disease detection in citrus, where the red-edge shift and reductions in SWIR reflectance were also observed under drought and other foliar diseases (Deng et al., 2019; He et al., 2022; Terentev et al., 2022). Such spectral convergence increases the risk of false positives when relying exclusively on reflectance data for HLB detection.

Considering this, the results do not suggest that leaf-level spectral data are inherently inadequate for characterizing HLB status. Rather, they underscore the importance of confirming the infection status of each leaf—ideally through PCR diagnostics.

3.3 Spectral Variability Among Bands at the Plant Level

Spectral variability within HLB-positive plants was notably higher, especially in the green to red-edge transition region (~550–1000 nm), with pronounced variance peaks also observed in the shortwave infrared (SWIR; 1500–1800 nm and 2000–2200 nm). This elevated variability corresponds to the spatial heterogeneity of symptom expression typically observed in HLB-infected plants (Porto, 2021). In contrast, healthy plants exhibited more uniform reflectance patterns, resulting in lower spectral variance across the same regions. These findings are consistent with the patterns illustrated in the preceding figures 9 and 10, where statistical differences between HLB-positive and HLB-negative groups were also concentrated in these wavelengths. Variance and standard deviation plots further emphasized this pattern, revealing significant dispersion among symptomatic leaves and confirming the non-uniform manifestation of disease-related physiological changes.

This contribution has been peer-reviewed. The double-blind peer-review was conducted on the basis of the full paper.
https://doi.org/10.5194/isprs-annals-X-3-W4-2025-255-2026 | © Author(s) 2026. CC BY 4.0 License.

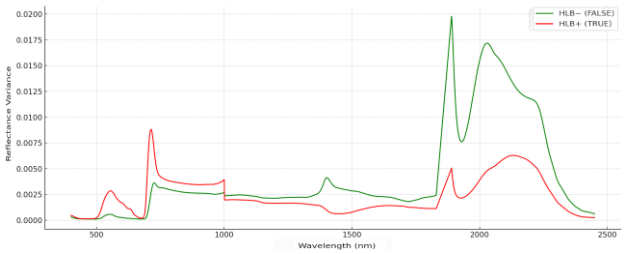

Figure 9 – Average spectral variance among individual leaves from HLB-positive and HLB-negative. The higher variability observed in HLB+ samples indicates heterogeneous symptom expression across the canopy.

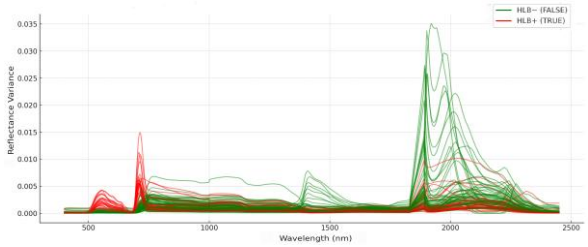

Figure 10 - Plant-level spectral variance for HLB-positive and HLB-negative groups, from all 89 citrus plants. Reduced variance in HLB-negative plants suggests physiological uniformity, while elevated variability in HLB-positive plants reflects spectral instability associated with disease.

The high spectral variance observed in HLB-positive plants, particularly in the transition region between the green and red-edge (approximately 550–750 nm), reflects the expected physiological instability associated with disease progression. This variability is consistent with the known spatial heterogeneity of HLB symptoms within the canopy. In contrast, HLB-negative plants exhibited considerably lower variance in the same spectral range, as expected for healthy and physiologically uniform individuals.

The analysis of variance across spectral bands reinforces the diagnostic potential of this region, as the increased variability in HLB-positive plants may serve as an indicator of early or uneven symptom expression. Such findings suggest that variance-based metrics, in addition to mean reflectance, can be valuable for identifying affected plants with non-uniform symptom distribution

3.4 Leaf-to-Plant Spectral Agreement in HLB-Positive Samples

To compare an individual infected leaf (i.e., a single observation) against a group of healthy leaves, a single-observation Z-test was applied. This test evaluates whether the spectral response of the individual leaf significantly deviates from the distribution of a reference group, using the group's mean and standard deviation for each spectral band.

While leaf-level spectra provide detailed physiological insights, they may limit the reliability of classification models due to the frequent occurrence of asymptomatic leaves within HLB-positive plants. Several studies have shown that HLB-infected trees often exhibit heterogeneous symptom expression across the canopy, resulting in leaves with spectral signatures similar to healthy tissues despite confirmed infection (Deng et al., 2019; Terentev et al., 2022). This mismatch between leaf-level labels and whole-plant infection status introduces potential biases during the training of machine learning algorithms, particularly when applied to UAV or satellite imagery where detection occurs at canopy scale.

The Z-test assumes that the spectral values of the reference group (HLB− leaves) follow a normal distribution, a prerequisite for ensuring the validity of the test results. By applying this method across all spectral bands, it was possible to determine whether the spectral signature of the infected leaf differed from that of the healthy group, thereby aiding in the detection of potentially misclassified cases.

Likewise, Khuimphukhieo et al. (2024) demonstrated that canopy-level aggregation using UAV spectral and structural metrics significantly improved classification robustness compared to single-leaf analysis, particularly when disease symptoms were spatially heterogeneous. These findings align with our observation that plant-level aggregation reduces intra-class variability, enhancing the reliability of spectral separability when scaled to orchard-level monitoring.

Following this analysis, the proportion of spectral bands with p-values greater than 0.05 was calculated, indicating the percentage of bands where no significant difference was found between the HLB+ leaf and the healthy reference distribution.

Leaves exhibiting a high proportion of bands with $p > 0.05$ were considered potential false positives, as their spectral profiles were not statistically distinguishable from those of healthy leaves. This finding highlights the intra-plant spectral variability commonly associated with HLB, figura 11.

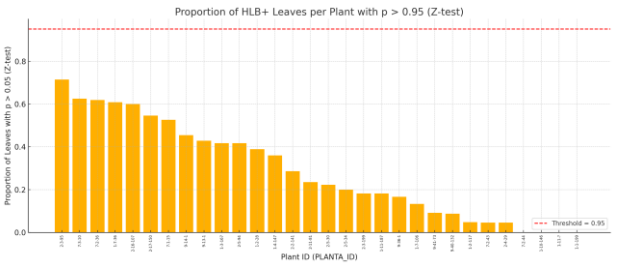

Figure 11 - Proportion of HLB-positive plants correctly represented by their leaf spectra versus those with inconsistent spectral signatures, based on Z-test (95% confidence). The results underscore the risk of misclassification when relying on individual leaves for disease detection.

Ideally, the spectral response of all 20 sampled leaves should collectively reflect the average physiological state of the plant—particularly with respect to the target variable. When this assumption is violated, it introduces a bias that can significantly affect the accuracy of classification models and the reliability of downstream analyses. The 177 HLB-positive leaves with more than 95% of spectral bands showing p-values greater than 0.05 (based on the Z-test) represent approximately 28.7% of all 617 HLB-positive leaves in the dataset.

These findings suggest that relying exclusively on individual leaves as ground truth may increase the risk of misclassification due to the inherent spectral variability within HLB-positive plants. However, it is important to weigh the practical implications of both analytical scales. Leaf-level analysis provides fine-grained physiological information, yet it is logistically demanding and may not be scalable for large-scale monitoring—particularly when considering the use of remote sensing platforms such as UAVs or satellite imagery. In

This contribution has been peer-reviewed. The double-blind peer-review was conducted on the basis of the full paper.
https://doi.org/10.5194/isprs-annals-X-3-W4-2025-255-2026 | © Author(s) 2026. CC BY 4.0 License.

contrast, plant-level aggregation offers a more feasible approach for operational disease detection in citrus orchards, especially when spectral characterization at the canopy level is required. Notably, in this study, both leaf- and plant-level analyses yielded similar discriminative patterns, reinforcing the validity of plant-level diagnostics. This convergence supports the deployment of hyperspectral sensing strategies that prioritize canopy-level assessments while maintaining diagnostic reliability.

3.5 Discriminative Spectral Regions

The discriminative spectral intervals identified in this study have direct operational relevance for remote sensing applications. The visible, red-edge, and SWIR regions—highlighted as the most robust for distinguishing HLB-positive from healthy plants—correspond to bands commonly available on UAV multispectral payloads and satellite sensors, such as Sentinel-2 and WorldView. These results enable the design of targeted vegetation indices and provide guidelines for selecting spectral configurations in hyperspectral and multispectral missions. Furthermore, by demonstrating the scalability of plant-level aggregation to canopy-level analysis, this study supports the integration of proximal spectral findings into orchard-level monitoring workflows, enhancing the feasibility of large-scale, non-invasive detection strategies.

Recent studies in hyperspectral disease detection have reported similar discriminative regions for Huanglongbing (HLB) and other citrus stresses, reinforcing the robustness of our findings. For instance, Ye et al. (2025) demonstrated that UAV-based multispectral imagery combined with deep learning achieved early detection of HLB by exploiting strong separability in the red-edge (705–783 nm) and SWIR (~1600–2200 nm) regions, consistent with the intervals identified in our study. Similarly, Porto et al. (2024) highlighted the potential of convolutional neural networks (ResNets) applied to terrestrial multispectral imaging, confirming that red-edge and NIR wavelengths are among the most diagnostic for differentiating symptomatic from asymptomatic tissues.

To overcome this limitation, recent advances have proposed the integration of complementary biomarkers to enhance disease specificity. For instance, fruit-level spectral features have shown greater diagnostic potential for distinguishing HLB from other stresses, as structural and biochemical changes in fruits often occur later in the infection process and are more directly linked to pathogen activity (Khuimphukhieo et al., 2024). However, fruit-based biomarkers are more challenging to capture via remote sensing because of occlusion by foliage and the low spatial resolution of orbital sensors. To address this, recent UAV-based studies have combined leaf-level and canopy-level reflectance with targeted sampling protocols to improve detection reliability (Ye et al., 2025; Porto et al., 2024).

To identify spectral regions most indicative of HLB infection, Welch's t-test and one-way ANOVA were applied at the leaf and plant levels, respectively. Welch's t-test was selected for the leaf-level analysis due to its robustness against unequal variances, which are often present in biological datasets. At the plant level, one-way ANOVA was employed to assess differences in mean reflectance, benefiting from reduced intra-plant variability through the aggregation of multiple leaf spectra per plant. These tests revealed statistically significant differences ($p < 0.05$) in reflectance between HLB-positive and HLB-negative citrus samples across multiple wavelengths, as illustrated in Figure 12.

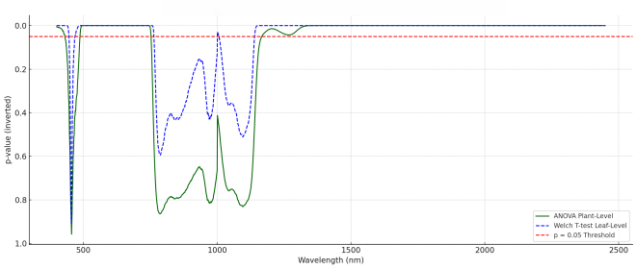

Figure 12 - Spectral bands with statistically significant differences ($p < 0.05$) between HLB-positive and HLB-negative citrus groups, as determined by Welch's t-test (leaf level, blue) and ANOVA (plant level, green). The convergence of discriminative wavelengths across both scales reinforces the robustness of spectral responses for HLB detection, regardless of the analytical level.

Figure 12 presents the spectral bands where significant differences were identified. The blue dashed line represents p-values from the Welch's t-test, while the green solid line corresponds to the ANOVA results. The red dotted line denotes the 0.05 significance threshold. While both tests highlighted meaningful discriminative bands, ANOVA revealed a broader range of significant wavelengths, particularly in the near-infrared (NIR; ~750–1300 nm) and shortwave infrared (SWIR; >1500 nm) regions. This suggests that plant-level aggregation improves the signal-to-noise ratio, enhancing the detection of consistent physiological differences associated with HLB infection.

The Welch's t-test identified fewer significant bands, primarily between 900 and 1100 nm, reflecting the higher variability in spectral data at the individual leaf level. However, there was notable overlap in the bands identified by both tests, particularly within the red and red-edge regions, indicating these spectral regions as robust indicators of HLB across both analytical scales.

Specifically, the tests highlighted four key spectral intervals with consistent discriminative potential: 400–431 nm, 488–752 nm, 1132–1830 nm, and 1890–2500 nm. These results support the hypothesis that spectral heterogeneity in HLB-positive plants limits the reliability of single-leaf diagnostics. Nevertheless, leaf-level analysis may still be effective when sampling strategies ensure the inclusion of symptomatic tissues—especially if PCR confirmation is used per leaf, which was not the case in this study, figure 13.

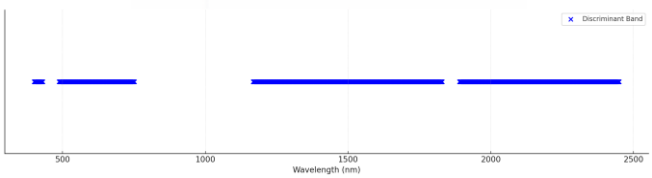

Figure 13 - Common discriminative wavelengths between leaf- and plant-level analyses that enable differentiation between HLB-infected and healthy citrus plants. These spectral regions are key candidates for developing targeted indices and sensor designs.

Thus, while plant-level spectral aggregation yielded more stable discrimination, both analytical levels demonstrated valuable contributions. The choice between them should consider factors such as sampling representativeness, scale of analysis, and sensor availability. Importantly, the discriminative bands

This contribution has been peer-reviewed. The double-blind peer-review was conducted on the basis of the full paper.
https://doi.org/10.5194/isprs-annals-X-3-W4-2025-255-2026

identified—particularly those in the red and red-edge regions—should be prioritized for the development of targeted vegetation indices and hyperspectral sensor designs for HLB detection.

Furthermore, recent advances demonstrate the feasibility of integrating plant-scale hyperspectral findings into satellite-based monitoring frameworks. Studies using Sentinel-2 multispectral data have successfully exploited red-edge (B5–B7, B8A) and SWIR (B11, B12) bands to map canopy health and detect early citrus stresses at regional scales (Della Bellver et al., 2024; Matese & Di Gennaro, 2024). These results underscore the operational potential of translating the discriminative bands identified here into large-scale monitoring protocols using medium- to high-resolution satellite imagery.

Promising approaches are emerging through multi-modal data fusion, integrating hyperspectral reflectance with fluorescence imaging, thermal signatures, and even LiDAR-derived canopy structure. For example, He et al. (2022) demonstrated that combining multicolour fluorescence with hyperspectral reflectance substantially improved HLB detection accuracy compared to single-sensor approaches. Similarly, Matese & Di Gennaro (2024) highlight that UAV-based hyperspectral platforms coupled with thermal imaging and high-resolution canopy models can differentiate HLB-induced stress from other abiotic disorders at orchard scale. These strategies are paving the way for next-generation remote sensing frameworks, improving both early detection and disease-specific classification.

4. Conclusions

The statistical analyses conducted in this study enabled a detailed spectral characterization of healthy and HLB-infected citrus plants at both the leaf and plant levels. By evaluating reflectance averages, variability, and the statistical significance of differences across spectral signature, it was possible to assess the consistency of spectral patterns between scales. We noted considerable intra-plant spectral variability in HLB-positive individuals, which may compromise the representativeness of leaf-level measurements in some cases. However, the overall agreement between leaf- and plant-level spectral behaviour—especially in key wavelength regions—indicates that both scales can provide complementary and convergent information for HLB detection. These findings highlight the potential of hyperspectral sensing as a valuable tool for disease monitoring, supporting the development of targeted sensors and vegetation indices based on statistically validated discriminative bands.

Aggregating reflectance data at the plant level reduced spectral dispersion and improved the separability between HLB-positive and HLB-negative groups, reinforcing the value of ensemble-based approaches. Discriminative spectral regions were consistently identified within four key intervals: 400–431 nm, 488–752 nm, 1132–1830 nm, and 1890–2500 nm. Notably, the first two ranges fall within the visible and red-edge domains, which are commonly associated with pigment-related changes. In contrast, the latter two intervals lie in the shortwave infrared (SWIR) region and are likely linked to structural and water-content differences between healthy and diseased tissues. These findings are highly relevant for the development of targeted vegetation indices and spectral filters optimized for early and accurate HLB detection.

To address potential biases introduced by asymptomatic leaves in model training, recent approaches have explored advanced machine learning strategies. For example, Ye et al. (2025) combined UAV multispectral imagery with deep learning models capable of capturing contextual canopy information, improving the robustness of detection in heterogeneous orchards. Similarly, Matese & Di Gennaro (2024) emphasized that incorporating temporal features from multi-date satellite imagery, especially red-edge and SWIR bands from Sentinel-2, can help distinguish early stress responses from healthy vegetation dynamics. These strategies demonstrate the importance of multi-scale data integration to improve classification performance and generalization capacity.

In summary, this study highlights the critical role of choosing an appropriate analytical scale in spectral disease detection workflows. While aggregation at the plant level yielded more consistent results, the general agreement between leaf- and plant-level analyses suggests that both approaches can offer valuable insights—depending on the sampling strategy and the representativeness of the collected data. Given the limited number of leaves per plant and the absence of PCR validation at the leaf level, further studies are recommended to validate the diagnostic robustness of each scale under different conditions. Future applications incorporating these insights may enhance the robustness and reliability of machine learning models and remote sensing platforms for citrus disease monitoring.

Acknowledgments

The authors would like to acknowledge the financial support of the *National Council for Scientific and Technological Development (CNPq, Brazil)* and the *Harpia Project (FAPESP, Brazil)*. We also gratefully thank *Embrapa Instrumentation (São Carlos, SP, Brazil)* for providing the datasets used in this research.

References

Castro, C., Giles, F., 2025: Update to Citrus Annual Report for Brazil, Brasilia, Brazil. United States Department of Agriculture (USDA), Foreign Agricultural Service. Report No. BR2025-0002, 06 February 2025.

Della Bellver, F., et al., 2024: Pest detection in citrus orchards using Sentinel-2. Remote Sensing, 16(23), 4362. https://doi.org/10.3390/rs16234362

Deng, X., et al., 2019: Field detection and classification of citrus HLB using hyperspectral reflectance. Computers and Electronics in Agriculture, 167, 105006. https://doi.org/10.1016/j.compag.2019.105006

Fisher, R.A., 1925: Statistical Methods for Research Workers. Oliver and Boyd, Edinburgh. Student, 1908: The probable error of a mean. Biometrika, 6(1), 1–25.

He, C., et al., 2022: Combining multicolor fluorescence imaging with hyperspectral reflectance for rapid HLB detection. Computers and Electronics in Agriculture, 194, 106808. https://doi.org/10.1016/j.compag.2022.106808

Jensen, J.R., 2009. Remote Sensing of the Environment: An Earth Resource Perspective. Pearson Education Limited, 2nd edition, London.

Khuimphukhieo, I., et al., 2024: Assessing HLB severity and canopy health with UAS features and ML in Texas orchards. Sensors, 24(23), 7646. https://doi.org/10.3390/s24237646

Martins, G.D., Galo, M.L.B.T., Vieira, B.S., 2017: Detecting and mapping root-knot nematode infection in coffee crop using remote sensing measurements. IEEE Journal of Selected Topics in Applied Earth Observations and Remote Sensing, 10(12), 5395–5403.

Matese, A., Di Gennaro, S.F., 2024: Are UAV-based hyperspectral imaging a game-changer for precision agriculture? Trends in Plant Science, 29(8), 780–793. https://doi.org/10.1016/j.tplants.2024.05.008.

Oliveira, A. S., 1999: O exemplo de Araraquara-SP. Revista Águas Subterrâneas, 13(1), 65–74. Weatherspark, 2025: Clima característico em Araraquara, São Paulo, Brasil durante o ano.

Orlando, V.S.W., Galo, M.d.L.B.T., Martins, G.D., Lingua, A.M., de Assis, G.A., Belcore, E., 2024: Hyperspectral characterization of coffee leaf miner (Leucoptera coffeella) (Lepidoptera: Lyonetiidae) infestation levels: a detailed analysis. Agriculture, 14(12), 2173.

Porto, L.R., 2021: Caracterização espectral da folha de Citrus contaminada por HLB baseado em espectrometria de campo. Master's thesis, Universidade Estadual Paulista "Júlio de Mesquita Filho", Presidente Prudente, SP, Brazil.

Porto, L.R., et al., 2024: Use of ResNets for HLB Disease Detection on Orange Leaves Using Terrestrial Multispectral Images. ISPRS Annals X-3-2024, 331–338. https://doi.org/10.5194/isprs-annals-X-3-2024-331-2024

Razali, N.M. and Wah, Y.B., 2011. Power comparisons of Shapiro-Wilk, Kolmogorov-Smirnov, Lilliefors and Anderson-Darling tests. Journal of Statistical Modeling and Analytics, 2(1), pp.21–33.

Shapiro, S.S., Wilk, M.B., 1965: An analysis of variance test for normality (complete samples). Biometrika, 52(3–4), 591–611. .
Terentev, A., et al., 2022: Current state of hyperspectral remote sensing for early plant disease detection: A review. Remote Sensing, 14(3), 561. https://doi.org/10.3390/rs14030561

Walpole, R.E., Myers, R.H., Myers, S.L., Ye, K., 2012. Probability and Statistics for Engineers and Scientists, 9th ed. Pearson Education, Boston.

Welch, B.L., 1947: The generalization of 'Student's' problem when several different population variances are involved. Biometrika, 34(1–2), 28–35.

Ye, N., et al., 2025: Early detection of Citrus Huanglongbing by UAV remote images using multispectral and deep learning. Frontiers in Plant Science, 16:1503645. https://doi.org/10.3389/fpls.2025.1503645.